

A stochastic model of Min oscillations in *Escherichia coli* and Min protein segregation during cell division

Filipe Tostevin and Martin Howard

Department of Mathematics, Imperial College London, London SW7 2AZ, UK

E-mail: filipe.tostevin@imperial.ac.uk

Abstract. The Min system in *Escherichia coli* directs division to the centre of the cell through pole-to-pole oscillations of the MinCDE proteins. We present a one dimensional stochastic model of these oscillations which incorporates membrane polymerisation of MinD into linear chains. This model reproduces much of the observed phenomenology of the Min system, including pole-to-pole oscillations of the Min proteins. We then apply this model to investigate the Min system during cell division. Oscillations continue initially unaffected by the closing septum, before cutting off rapidly. The fractions of Min proteins in the daughter cells vary widely, from 50%-50% up to 85%-15% of the total from the parent cell, suggesting that there may be another mechanism for regulating these levels *in vivo*.

PACS numbers: 87.16.Ac, 87.17.Ee, 05.40.-a

Submitted to: *Phys. Biol.*

Keywords: cell division, *Escherichia coli*, MinD, MinE, centre finding

1. Introduction

Reproduction of the rod-shaped bacterium *Escherichia coli* takes place through binary fission. In order for the production of viable daughter cells the site of division must be accurately located at the middle of the cell to ensure one chromosome is distributed to each daughter cell. This positional information is provided by the combined action of nucleoid occlusion, which inhibits division close to the chromosomes, and the proteins of the Min system. Investigation of the dynamics of the Min proteins has decisively shown that mathematical modelling and ideas from pattern-formation can be useful in the study of subcellular processes [1].

Cell division occurs after the chromosome has been replicated and the daughter chromosomes have moved into opposite halves of the cell. Nucleoid occlusion limits division to regions without DNA [2], i.e. the cell's centre or poles. The Min system consists of the proteins MinC, MinD and MinE. Its function is to prevent septal ring formation at the cell poles, so the only favourable division site is at the cell centre, equidistant from the two cell poles.

In the presence of MinE, the MinC and MinD proteins oscillate between the two cell poles [3, 4]. MinC and MinD are observed to occupy the membrane in one half of the cell. A MinE ring forms at the medial end of this region and moves towards the cell pole [5, 6], displacing the MinC and MinD in the process. The MinC and MinD then gather in the opposite half of the cell, and the process repeats. The period of these oscillations *in vivo* is 30-120 seconds.

Several studies have been made with different reaction-diffusion models to explain these oscillations [7, 8, 9, 10, 11]. Subsequent experiments have investigated the reaction steps involved in the Min oscillation cycle, and have allowed the details of the models to be refined: MinD:ATP first binds to the cell membrane. In the absence of MinE, MinD is distributed evenly throughout the membrane [3]. The rate of MinD accumulation, through cooperative binding or self-aggregation, increases with the amount of MinD present [12]. MinD forms oligomers [13, 14], and can form a complex with either MinC or MinE [15]. MinC inhibits polymerization of FtsZ [16], preventing formation of the "Z-ring" which forms the basis for the division machinery. MinD enhances the effect of MinC by recruiting it to the membrane. MinC is co-localized with membrane-bound MinD [4, 17]. However, MinC is not required for the oscillation of MinD and MinE [3]. MinE is recruited to the membrane by MinD where it forms a MinDE complex and, in the process, expels MinC from the membrane [12]. MinE also stimulates ATP-hydrolysis of membrane-bound MinD, which causes dissociation of MinD from the membrane. MinD:ADP then undergoes nucleotide exchange in the cytoplasm to MinD:ATP.

It has also recently emerged that MinD forms helical filaments in living cells [18]; recent mathematical models [19, 20, 21] have attempted to include this feature. In the Meacci-Kruse model [20] the membrane occupancy is limited, and MinD accumulation is due to self-aggregation once it has bound to the membrane. The model by Drew *et al* [19] includes polymer growth from nucleation sites at the ends of the cell, but

this and other assumptions upon which it relies, such as regulating polymer growth rate according to length, are not required in other models. Both of these models use continuous partial differential equations. The model by Pavin *et al* [21] differs in that it is a three-dimensional stochastic model, but it does not form the observed large scale helical filaments. Incorporating stochasticity (first introduced into Min modelling in [10]) is nevertheless likely to be important for systems of this type: for example, fluctuations are believed to be vital for modelling the closely related Spo0J/Soj dynamics in *Bacillus subtilis* [22].

In this paper, we present a simple one-dimensional stochastic model that reproduces many of the experimental observations of the Min oscillations. Aside from including full fluctuation effects, our stochastic model tracks individual protein particles, and thus makes it easier to, (i), incorporate the structure of the Min proteins on the membrane, (ii), limit the maximum membrane occupancy, and, (iii), allow binding rates to depend on the local arrangement of the proteins. Importantly, we allow the MinD to form linear membrane-bound polymers along the cell length. However, as we will see, oscillatory dynamics can be reproduced independent of many of the details of the polymer structure. In our model we have therefore chosen a particularly simple implementation of membrane polymerisation. We also assume that proteins incorporated into membrane-bound polymers are fixed in place and cannot diffuse. This difference in mobility between the membrane and cytoplasm is crucial for enabling pattern formation in our model.

Although the Min oscillations have been studied in detail, there have only been a few comments describing oscillations in constricting and recently divided cells [3, 4]. We therefore use our model to investigate the Min system during these phases by incorporating division at the centre of the cell into the simulations. We find that the dynamics of the Min proteins during contraction of the Z-ring is generally consistent with the available experimental observations: the pole-to-pole oscillations continue for some time and then the dynamics changes sharply to independent oscillations on each side of the septum. We also study the numbers of Min proteins that are found in the two daughter cells. The numbers of Min proteins in each half of the parent cell vary greatly over the pole-to-pole oscillation period, and we find that the protein numbers in the daughter cells also vary from cell to cell over a similar range. This result suggests that the number of Min proteins may fluctuate strongly from cell to cell, but also that there may be other mechanisms for controlling protein numbers *in vivo*, such as the rates of Min protein synthesis being regulated by the Min protein concentration levels.

2. The Model

The cell is modelled in 1-dimension by dividing the length L into N discrete intervals of width $dx = L/N$. Each interval i contains n_p^i of each of the five protein states in the model. These are cytoplasmic MinD:ADP ($p = D : ADP$), cytoplasmic MinD:ATP ($p = D : ATP$), cytoplasmic MinE ($p = E$), membrane-bound MinD ($p = d$), and

membrane-bound MinDE complex ($p = \text{de}$). MinE is present as a homodimer [23], so one MinE unit is actually a dimer rather than a single protein. Experiments show that MinC is not required for the oscillations, so it is not included explicitly in the modelling. Since MinC is co-localized with MinD in a MinCD complex, we assume that the amount of membrane-bound MinC can be quantified by measuring n_d^i . In our simulations we use a time step dt . Simulations begin with either uniform initial protein distributions or random distributions without affecting our results.

Membrane filaments are modelled by subdividing the cell membrane into N_c linear arrays of n_{max} possible binding sites for each of the N discrete intervals. Each of the N_c arrays extends along the length of the cell, allowing filaments to grow regardless of the discretization boundaries in the cytoplasm. During the reaction steps, cytoplasmic molecules may bind to membrane sites contained within the interval they currently occupy, as shown in figure 1. Each of these membrane sites influences only its immediate neighbours on the membrane, and any molecules occupying neighbouring sites are considered bound in a polymer chain. The dynamical behaviour is independent of the values of N_c and n_{max} provided the total number of membrane binding sites per cytoplasmic site, $N_c n_{\text{max}}$, is maintained. This result suggests that the overall number of MinD molecules that can bind to the membrane influences the dynamical behaviour, but the number of filaments into which they are arranged does not.

In this paper we employ a particularly simple way to incorporate polymerisation, with a minimal number of assumptions about the *in vivo* polymerisation and structure. Since we can reproduce the Min oscillations with this model, the exact details of polymerisation appear not to be important for generating the experimentally observed Min dynamics. In particular we include only the basic effects which any more advanced polymerisation model must also contain, the most important of which is reduced mobility for proteins which are membrane bound. In the model, once bound to the membrane a molecule cannot move and is fixed in place until it dissociates from the membrane. We have also tested the model with diffusion of isolated membrane MinD with a similar diffusion constant to that in the cytoplasm. This change has no effect on the behaviour of the model as the amount of isolated membrane MinD is small compared to the amount of membrane MinD bound together into polymers.

All cytoplasmic proteins diffuse with diffusion constant D . The probability of a molecule moving to the left or right,

$$n_p^i \rightarrow n_p^i - 1, \quad n_p^{i\pm 1} \rightarrow n_p^{i\pm 1} + 1, \quad (1)$$

in a time interval dt is $Ddt/(dx)^2$.

MinD:ATP binds to the cell membrane:

$$n_{\text{D:ATP}}^i \rightarrow n_{\text{D:ATP}}^i - 1, \quad n_d^i \rightarrow n_d^i + 1. \quad (2)$$

Cooperative binding and self-assembly of MinD are simulated by using two different rates for membrane attachment. If a MinD molecule is present on the membrane and a neighbouring membrane site is empty, cytoplasmic MinD:ATP will bind with probability $\sigma_{\text{d,coop}} dt$ for each such site. MinD may also bind to any other empty site with a much

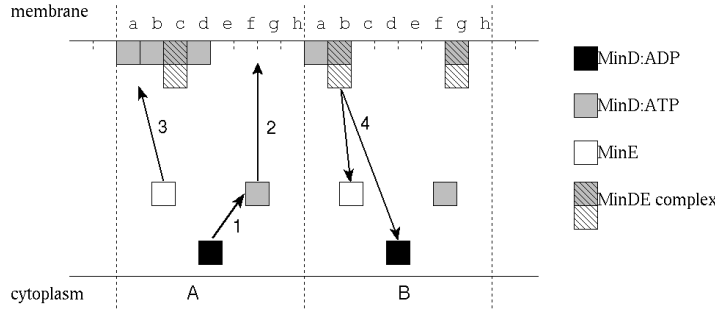
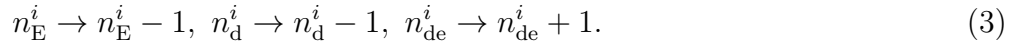


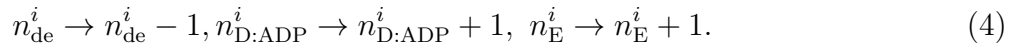
Figure 1. Schematic showing the model steps with one membrane filament ($N_c = 1$), with $n_{\max} = 8$: 1. MinD:ADP converts to MinD:ATP. 2. MinD:ATP binds to the membrane. In this case, a MinD:ATP in cytoplasmic site A could bind at membrane position Ae or Ah with probability $\sigma_{d,\text{coop}}dt$, or at Af or Ag with probability $\sigma_{d,\text{sp}}dt$. MinD:ATP in cytoplasmic site B could bind with the lower probability to each empty site as there are no suitable sites for cooperative binding. 3. MinE binds to membrane MinD with probability $\sigma_e dt$ per binding site. 4. The MinDE complex dissociates, giving cytoplasmic MinD:ADP and MinE. The complex would unbind from site Bg with probability $\sigma_{\text{dis,iso}}dt$, since both neighbouring sites are empty; from Bb with probability $\sigma_{\text{dis,end}}dt$; and from Ac with probability $\sigma_{\text{dis,bulk}}dt$, since both neighbouring sites are occupied.

lower probability, $\sigma_{d,\text{sp}}dt$. Since the binding rate is much higher if there is already MinD on the membrane, polymer chains form as protein particles preferentially bind to the MinD already present. In the model, MinD is not allowed to bind cooperatively to the MinDE complex. If this reaction is allowed to take place at the faster rate $\sigma_{d,\text{coop}}$, then oscillations do not occur. MinD is allowed to bind adjacent to the MinDE complex, but at the slower rate $\sigma_{d,\text{sp}}$. We consider that MinE at the end of a polymer blocks the tendency for self-assembly, but cannot completely block MinD binding.

Cytoplasmic MinE may bind to a membrane-bound MinD molecule, with probability $\sigma_e dt$ for each such site, forming the MinDE complex:



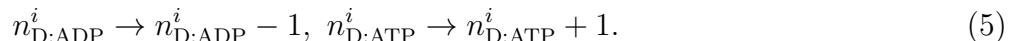
Dissociation of the complex releases one MinD:ADP molecule and one MinE dimer into the cytoplasm:



There are three rates for dissociation, depending on the position in the membrane array. The fastest rate and hence highest probability, $\sigma_{\text{dis,iso}}dt$, is for isolated molecules of the MinDE complex, which have no immediate neighbours on the membrane. The complex unbinds from the end of a chain (i.e. if it has one empty neighbouring site) with lower probability $\sigma_{\text{dis,end}}dt$, and from within a chain (neither neighbouring site empty) with a still lower probability $\sigma_{\text{dis,bulk}}dt$. These slower rates result from the existence of bonds to neighbouring units in the polymer chain. However, these different rates are not required for the oscillations, which can be achieved with a single dissociation rate independent of position. This suggests that the cooperative binding and reduced mobility introduced

by polymerisation are more important in generating oscillations than the details of disassembly. However, we still include these three rates to take account of the polymer nature of the membrane proteins.

MinD is released from the membrane in the MinD:ADP form. Before it is able to rebind it must undergo nucleotide exchange to the MinD:ATP form:



This occurs in an interval dt with probability $\sigma_{\text{DT}}dt$. This reaction step is also not required for the oscillations, but its inclusion makes the model more robust to changes in protein numbers.

2.1. Parameters

We use $dx = 0.01\mu\text{m}$ and $dt = 10^{-5}\text{s}$. We have checked that reducing dt by a factor of 10, or reducing dx by a factor of 4 while keeping L and the total number of membrane sites constant, does not affect our results. We take $N_c = 2$ since observations suggest that there are about two independent helical MinD filaments in living cells [18]. In our model there is no interaction between different filaments, since they are likely to be spaced far apart on the cell membrane. MinD proteins have a length of approximately 5nm [14]. Assuming that during polymerisation there is some overlap or interlocking, and that the helical filaments have a relatively large angle with the cell's long axis [18], we assume it takes 6 MinD molecules to span the $dx = 0.01\mu\text{m}$ interval. Furthermore, MinD polymers are likely to be double-stranded [14], and we have therefore taken $n_{\text{max}} = 2 \times 6 = 12$. However, we have observed oscillations for $N_c n_{\text{max}}$ in the range 12-30 and N_c from 1 to 4, indicating a high degree of robustness in the values of these parameters. For smaller $N_c n_{\text{max}}$ values, MinD fails to form the high density polar regions required for oscillation, instead filling the membrane uniformly. For larger $N_c n_{\text{max}}$, large amounts of MinD are able to gather in small regions, and as a result regions of high MinD concentration are not observed to extend long distances across the cell.

Unless otherwise specified, simulations are performed with $L = 3\mu\text{m}$. The densities used are $\rho_{\text{D}} = 1000\mu\text{m}^{-1}$ MinD protein particles and $\rho_{\text{E}} = 400\mu\text{m}^{-1}$ MinE homodimers [24]. We use $D = 2.0\mu\text{m}^2\text{s}^{-1}$, from experimental measurements of the diffusion rates of (unrelated) cytoplasmic proteins in *E. coli* [25]. The other parameters take the following values: $\sigma_{\text{DT}} = 1\text{s}^{-1}$, $\sigma_{\text{d,sp}} = 0.005\text{s}^{-1}$, $\sigma_{\text{d,coop}} = 30\text{s}^{-1}$, $\sigma_{\text{e}} = 50\text{s}^{-1}$, $\sigma_{\text{dis,iso}} = 10\text{s}^{-1}$, $\sigma_{\text{dis,end}} = 0.3\text{s}^{-1}$, and $\sigma_{\text{dis,bulk}} = 0.1\text{s}^{-1}$.

These values were chosen to fit the results of the model with experimental results, particularly the oscillation period. Increasing σ_{DT} increases the period, since MinD is able to rebind more quickly and will therefore rebind more times within one polar zone before diffusing to the opposite pole of the cell. $\sigma_{\text{dis,end}}$ controls the rate at which MinD polar zones are disassembled, and hence also has a significant effect on the period. However, the fundamental oscillatory dynamics are robust to significant changes in each of the parameter values individually. For example, oscillations persist if $\sigma_{\text{d,coop}}$ or σ_{e} are changed by a factor of 2. The values of $\sigma_{\text{dis,bulk}}$, $\sigma_{\text{dis,iso}}$ and $\sigma_{\text{d,sp}}$ have little effect on

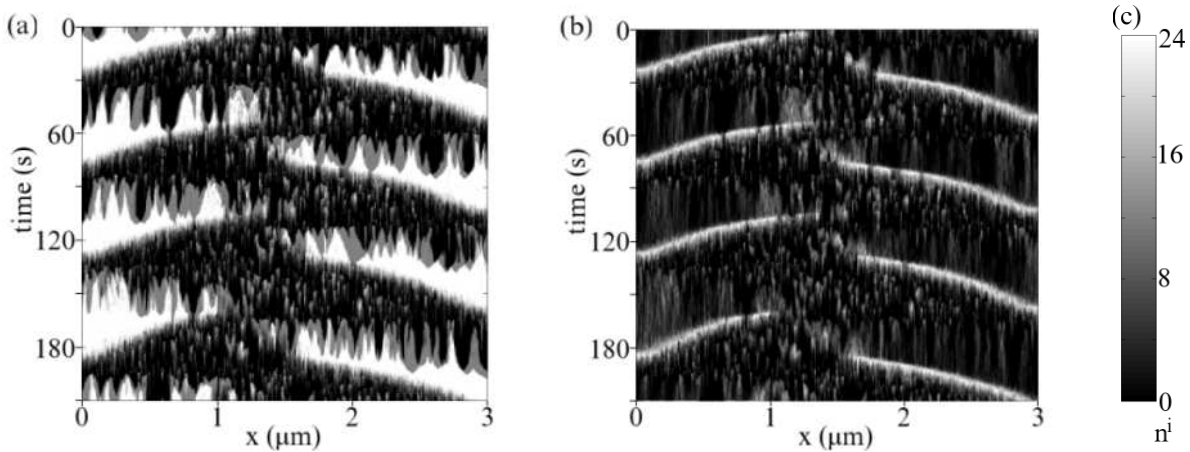


Figure 2. Space-time plot of protein densities for (a) membrane-bound MinD, and (b) the MinDE complex; (c) shows the scale used.

the dynamics, as long as $\sigma_{d,sp} \ll \sigma_{d,coop}$, although increasing $\sigma_{d,sp}$ or decreasing $\sigma_{dis,iso}$ does lead to increased noise in the oscillatory pattern.

2.2. Results

Pole-to-pole oscillations: Initially there is a transient period which lasts about one to two minutes, during which pole-to-pole oscillations are established. After this time, the oscillations are stable and persist over at least 90 minutes of simulated time.

In our model, MinD filaments tend not to grow out from the cell poles, instead the MinD filaments grow from random sites in the half of the cell where the concentration of MinE is lower. This is in contrast with experiment, where MinD polar regions often grow from the cell pole towards midcell. This difference in behaviour is a general feature of our model, independent of specific parameter values. In particular, it is difficult to prevent binding away from the cell pole because the MinE levels are low and roughly constant over this region. A more significant change to the model, such as adding favourable binding sites near the cell poles, could perhaps overcome these difficulties.

When a polymer has a chance to form in a region with little MinE, fast cooperative binding means the polymer grows rapidly in both directions, towards the centre and the pole of the cell. MinD polymers in regions with high MinE concentrations do not grow to a significant length, as the MinE prevents further cooperative binding and causes dissociation from the membrane. From figures 2 and 3 we can see that near mid-cell there are a large number of small patches of MinD, which are short in length and short-lived. These are quickly occupied by MinE and displaced from the membrane. Figure 3 shows that the pattern of each individual filament follows that of both filaments taken together.

As MinE relocates from the other end of the cell by cytoplasmic diffusion, it will tend to bind to the membrane at the first encountered region of elevated MinD concentration. Hence, as can clearly be seen in figure 2(b), a tightly localized region

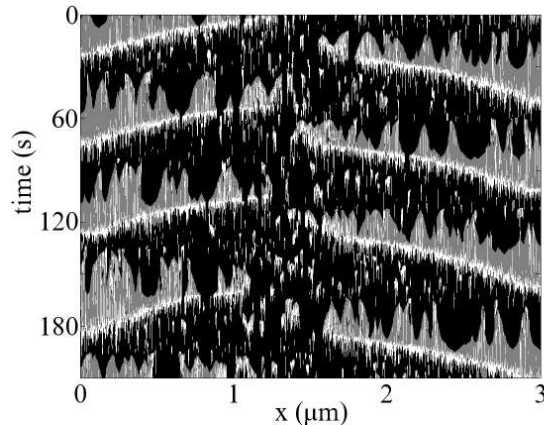


Figure 3. Space-time plot for occupancy of a single membrane filament with $n_{\max} = 12$ and $N_c = 2$. Black areas are empty, gray shows MinD and white is the MinDE complex.

of high MinE concentration (the “MinE ring”) typically accumulates at the end of the region of high MinD concentration. Since MinD forms polar zones, the MinE ring is nucleated close to mid-cell and thereafter moves towards the pole, via detachment, diffusion and reattachment, as the MinD region shrinks. Although the different filaments are independent, they are disassembled simultaneously since MinE binds equally to each.

Time-averaged concentrations: Oscillation cycles were identified as periods between the MinE ring reaching one cell pole. This was done manually by looking at n_{de}^1 , identifying times where the occupancy was high for an extended period, and defining the end of the cycle as the time when the occupancy dropped to below $N_c n_{\max}/2$. For each of the Min proteins, the membrane density as a function of position was averaged over each oscillation cycle. Figure 4 shows the mean and standard deviation of these profiles over a large number of oscillation cycles. We can see that fluctuations in our stochastic model do not destroy the biologically important midcell concentration minima for MinC and MinD.

The key result for cell division is that the concentration of MinC (which in our model is quantified by n_{d}^i) is maximized at the ends of the cell, suppressing Z-ring formation at these locations. The total amount of membrane-bound MinD, including the MinDE complex ($n_{\text{d}}^i + n_{\text{de}}^i$), also has a minimum around the cell centre and maxima at the cell ends. This result is in good agreement with experimental observations [20]. In our model, the average amount of membrane-bound MinE is roughly constant along the length of the cell, although with large fluctuations. This contrasts with other models which have a minimum [9, 11, 20, 21] or maximum [8] for membrane MinE at the cell centre. This profile has not been measured experimentally. Such a measurement could potentially distinguish between the various models.

Variation of period with protein numbers: Figure 5 shows that the oscillation period increases with increasing MinD concentration, and decreases with increasing MinE concentration. This is consistent with experimental observations [3]. The range

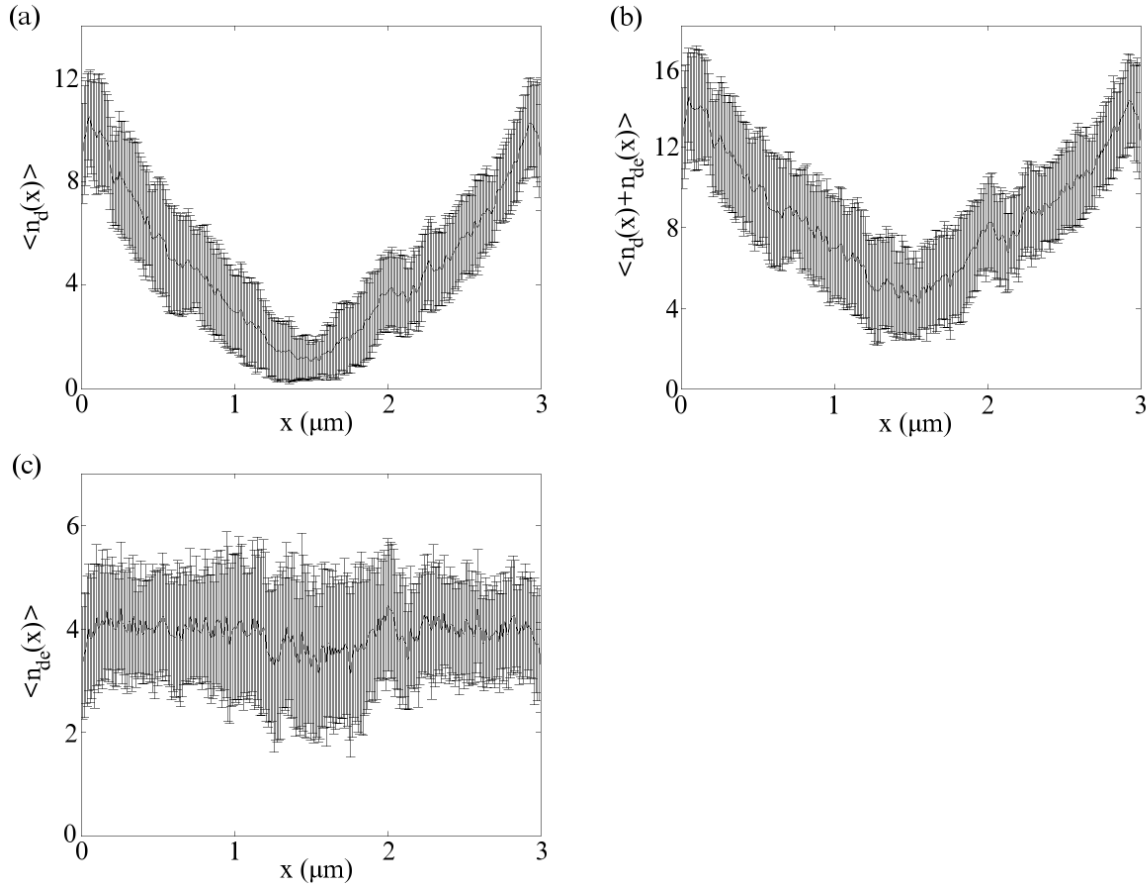


Figure 4. The time-averaged amount and oscillation-to-oscillation variability of (a) MinD not including the MinDE complex, (b) total MinD and (c) MinDE present on the membrane as a function of position along the cell. See text for details of the averaging procedure.

of periods supported in this model also covers that observed *in vivo*, where the variation is likely due to the fluctuations in protein copy numbers between different cells.

Oscillations occur for a fairly large range of $\rho_D : \rho_E$ ratios, but cut off when the $\rho_D : \rho_E$ ratio drops below about 1.6. At these concentration levels, MinD filaments are unable to grow to a significant length because they are removed from the membrane too quickly. At the opposite end of this scale there is no sharp transition; increasing $\rho_D : \rho_E$ causes the polar zones to extend further into the opposite half of the cell. Above the range shown in figure 5(a), the “polar zone” effectively extends for the whole length of the cell and MinE is unable to empty the membrane.

Filamentous cells: Observations of filamentous cells which are unable to divide have revealed regularly spaced bands of MinD with accompanying MinE rings [3, 5, 6]. This is strong evidence in favour of a dynamic instability mechanism for the oscillations, since the presence of bands supports the existence of a characteristic wavelength for the dynamics independent of the cell length. Figure 6 shows the results of simulations of our model performed in longer cells. In some cases, periodic oscillations with a number of

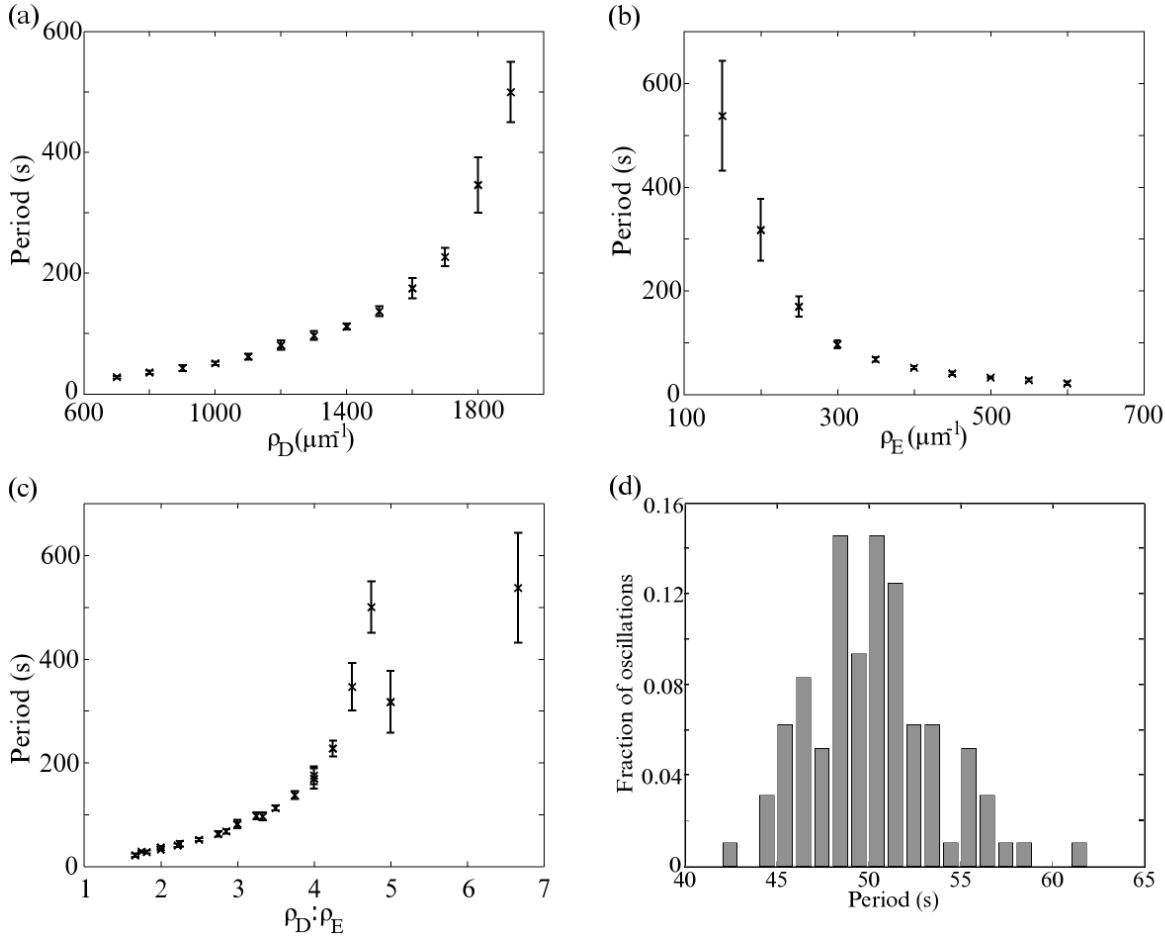


Figure 5. Variation of oscillation period when varying (a) ρ_D with $\rho_E = 400\mu m^{-1}$, (b) ρ_E with $\rho_D = 1000\mu m^{-1}$, and (c) $\rho_D : \rho_E$ ratio. (d) Distribution of 100 periods for the case with $\rho_D = 1000\mu m^{-1}$ and $\rho_E = 400\mu m^{-1}$. The distribution is similar in other cases. In those cases where the observed period is less than about 100s, the standard deviation is always close to 10% of the period.

MinD bands are observed, with the number of bands increasing with the cell length. In other cases, several regularly spaced bands form, but these all advance towards the same cell pole. In these cases the dynamics is more disordered. Such disordered behaviour has not yet been reported experimentally. However our model predicts that, while periodic behaviour may be seen over some intervals of up to 30 minutes, many filamentous cells will also have periods of irregular dynamics or switch between single and double banded oscillations. Such irregularity is perhaps not surprising given the stochastic nature of our model, and would certainly be interesting to search for experimentally.

Variation of period with length: Figure 7 shows the variation of oscillation period with cell length, while keeping the protein concentrations constant so the total protein number increases proportional to L . Over the range $1\mu m \leq L < 6\mu m$, where only single banded pole-to-pole oscillations are observed, the period remains approximately constant as the length is varied. Experimental evidence [20] is that any change in the

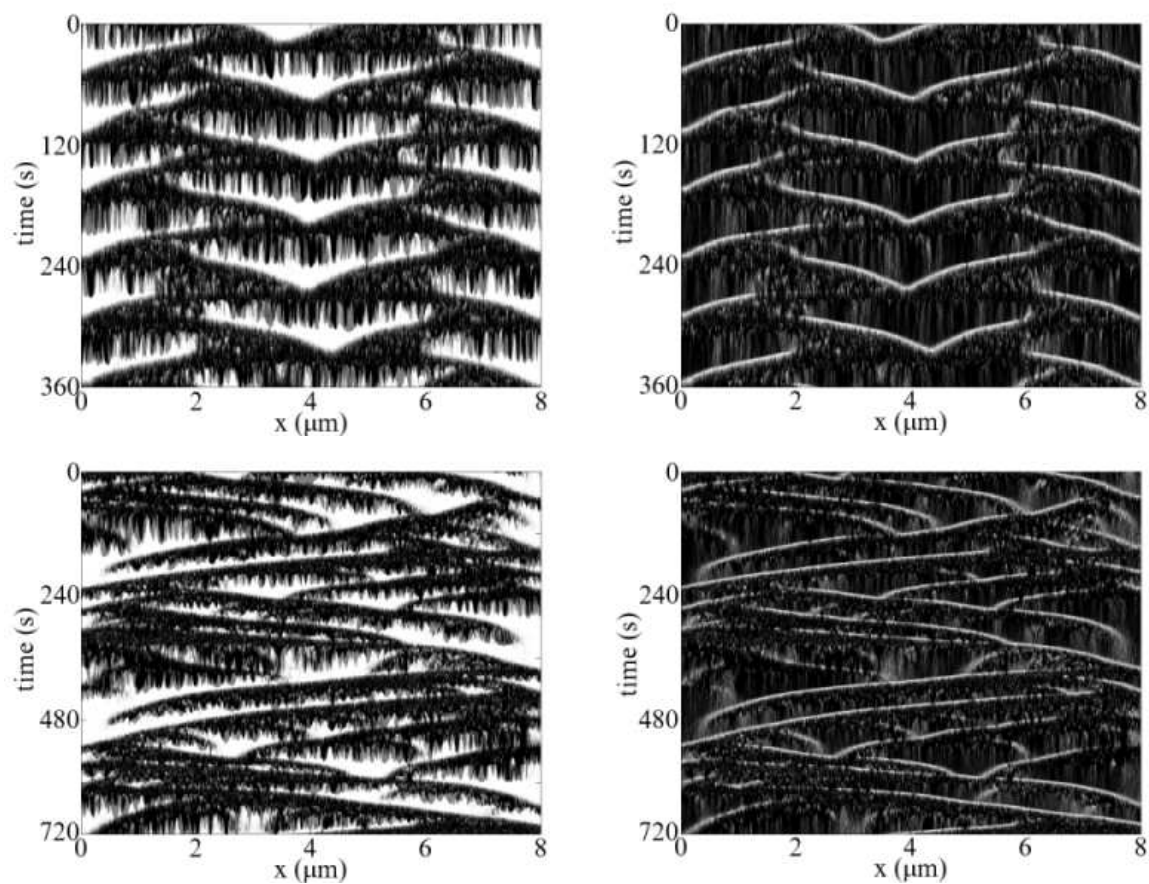


Figure 6. Membrane occupancy in $8\mu\text{m}$ cells, showing both periodic and more disordered dynamics. Plots on the left show membrane MinD. Plots on the right show the corresponding MinDE complex distribution.

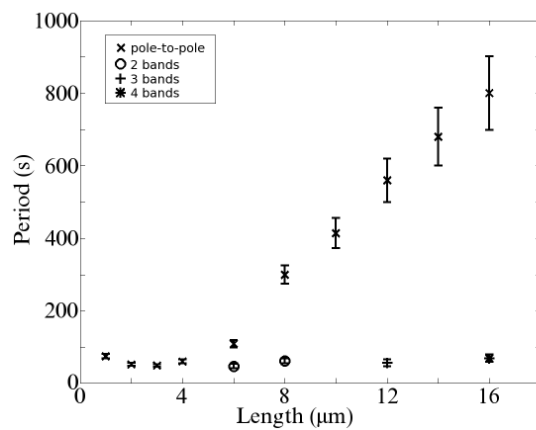


Figure 7. Variation of period with cell length, L .

period with length *in vivo* is much smaller than the variation in period at constant length, which is presumably due to concentration levels differing between individual cells. When multiple oscillation bands are observed in longer cells, beginning at about $L = 6\mu m$, their period is similar to that of the pole-to-pole oscillations in shorter cells.

In the case of disordered behaviour it is more difficult to identify a characteristic period in the observed dynamics. However, the dynamics is often dominated by the bulk of the MinD sweeping regularly from one pole to the other, and we use this to find the dominant period of oscillation. For example in the lower panels of figure 6, $t = 230s$ to $t = 530s$ would be considered to be one period. The period of this type of oscillation increases linearly with cell length, in contrast to the roughly constant period observed for $L < 6\mu m$.

We believe this difference in behaviour is the result of two qualitatively different types of dynamics. In short cells continuous MinD zones form between the cell pole and the MinE ring at midcell. These polar zones have a characteristic time associated with their disassembly regardless of cell length, which gives rise to the constant period of these oscillations. In long cells, the pole-to-pole oscillations are made up of MinD bands at intervals of $3 - 4\mu m$ that migrate across the cell through disassembly on one side and growth on the other. These bands always move at a particular speed, giving the linear increase in period with cell length.

However, the linear relationship intersects the L -axis at approximately $L = 4\mu m$. MinD bands in long cells travel less than the full length of the cell, because they form slightly away from the previously occupied pole and because once these MinD bands approach the other cell pole, polar zones similar to those in short cells form. So we can consider the oscillation period in long cells to be made up of two parts: the time to disassemble the polar zones, which is the oscillation period in short cells, plus the time taken for the MinD bands to travel twice across about $(L - 4)\mu m$ of the cell.

3. Oscillations during cell division

Now that we have established that our model reproduces the *in vivo* behaviour of the Min system, we use the model to investigate the Min dynamics during cell division. We investigate two mechanisms to simulate the closing septum, and examine how the Min oscillations are altered both during this process and once the daughter cells have separated. In particular we would like to study the distribution of the numbers of the Min proteins in each daughter cell, as this has not yet been measured experimentally.

Model A: Let t be the time since invagination began and T be the total time from when invagination begins to when there is no longer a cytoplasmic connection between the daughter cells. Over a length, $2l$, centred at $x = L/2$, we assume that the invagination of the cell membrane causes “compression” of the cytoplasm, making diffusion more difficult. As a result of this compression, diffusion decreases to zero in this region by time T , and unless otherwise stated we assume that this decrease occurs quadratically with time. In model A, we therefore employ a reduced diffusion

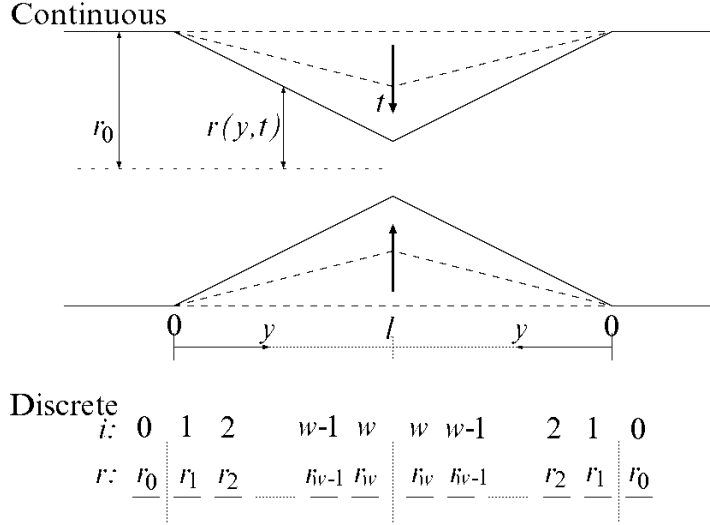


Figure 8. Schematic of the Model B septal region.

probability, $D'(t)dt/(dx)^2$, in the region $L/2 - l \leq x \leq L/2 + l$ with

$$D'(t) = D_0 \left(\frac{T-t}{T} \right)^2, \quad (6)$$

and where D_0 is the cytoplasmic diffusion constant in the rest of the cell.

Model A provides a simple way to implement the division process. However it is perhaps unrealistic to assume that diffusion is reduced equally over the whole range $2l$, particularly as there is little clear evidence for this “compression” of the cytoplasm. This model also neglects the importance of the direction of diffusive motion, whether towards or away from the septum and into a narrower or wider region. We therefore also investigate a second, possibly more realistic, model.

Model B: Figure 8 shows a schematic of this mechanism. Let y be the distance from the outer edge of the narrowing region measured towards the centre. We assume that the cell radius decreases linearly with y , and that the radius closes linearly with time:

$$r(y, t) = r_0 \left(1 - \frac{y t}{l T} \right). \quad (7)$$

Equation (7) discretizes to give

$$r_i(t) = r_0 \left(1 - \frac{i-1}{w} \frac{t}{T} \right), \quad i \geq 1. \quad (8)$$

where w is the number of sites in the contracting region and i is the site number counting from the polar end of this region. The presence of the -1 in the numerator simply reflects a choice in the discrete model of precisely where the invagination begins in space. The probability of diffusing into the next site towards the cell centre is assumed to vary with the ratio of the cross-sectional areas A_i , where $A_i \propto r_i^2$, since the narrowing cell radius may restrict the mobility of protein particles close to the membrane. This is equivalent to reducing the diffusion probability towards the septum from site i to site

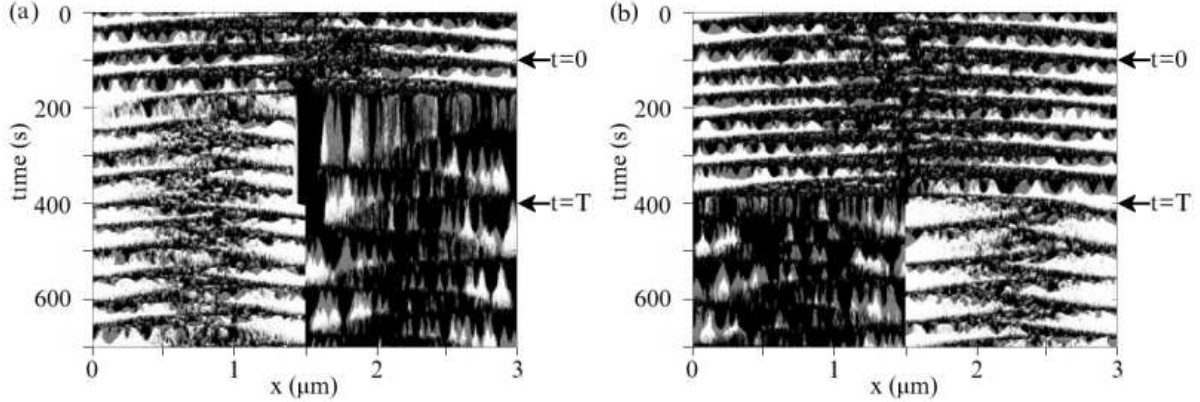


Figure 9. Space-time plot showing MinD oscillations in a dividing cell, for (a) model A and (b) model B. The division process begins at the point marked $t = 0$ and ends at $t = T$. The grey-scale used is the same as in figure 2.

$i + 1$, $D_i(t)dt/(dx)^2$, according to

$$\begin{aligned} D_i(t) &= D_0 \frac{A_{i+1}(t)}{A_i(t)} \\ &= D_0 \frac{\left(1 - \frac{i}{w} \frac{t}{T}\right)^2}{\left(1 - \frac{i-1}{w} \frac{t}{T}\right)^2}, \quad i = 1, \dots, w. \end{aligned} \quad (9)$$

The probability of diffusion away from the septum is unchanged at $D_0 dt/(dx)^2$.

Unless otherwise stated we use $T = 300s$ and $l = 0.1\mu m$ (estimated from [26]) or $w = 10$.

3.1. Results

Oscillations are initially unaffected as diffusion through the septum is reduced. Then at some later time diffusion through the septum cuts off sharply. After this time the two daughter cells are effectively independent, even though there remains a connection through the cytoplasm. This cut-off time varies between models but is approximately independent of the density distributions at $t = 0$. In model A, pole-to-pole oscillations cease relatively quickly, after approximately one minute. In model B, where the diffusion rate is on average greater because of the additional spatial variation, oscillations continue with little obvious alteration for about 270 seconds.

At the centre of the cell there is a region where the membrane remains empty, which appears at about the time when pole-to-pole oscillations are disrupted. Possibly the reduced diffusion probability makes it less likely that any proteins will be able to enter these sites, and thus reoccupy the membrane. For model A this includes about half of the contracting region, as can be clearly seen in figure 9(a). At $t = T$ the empty central region is quickly reoccupied because we restore the diffusion rate to D_0 (except at $x = L/2$) and proteins can once again access these sites. For model B, the empty

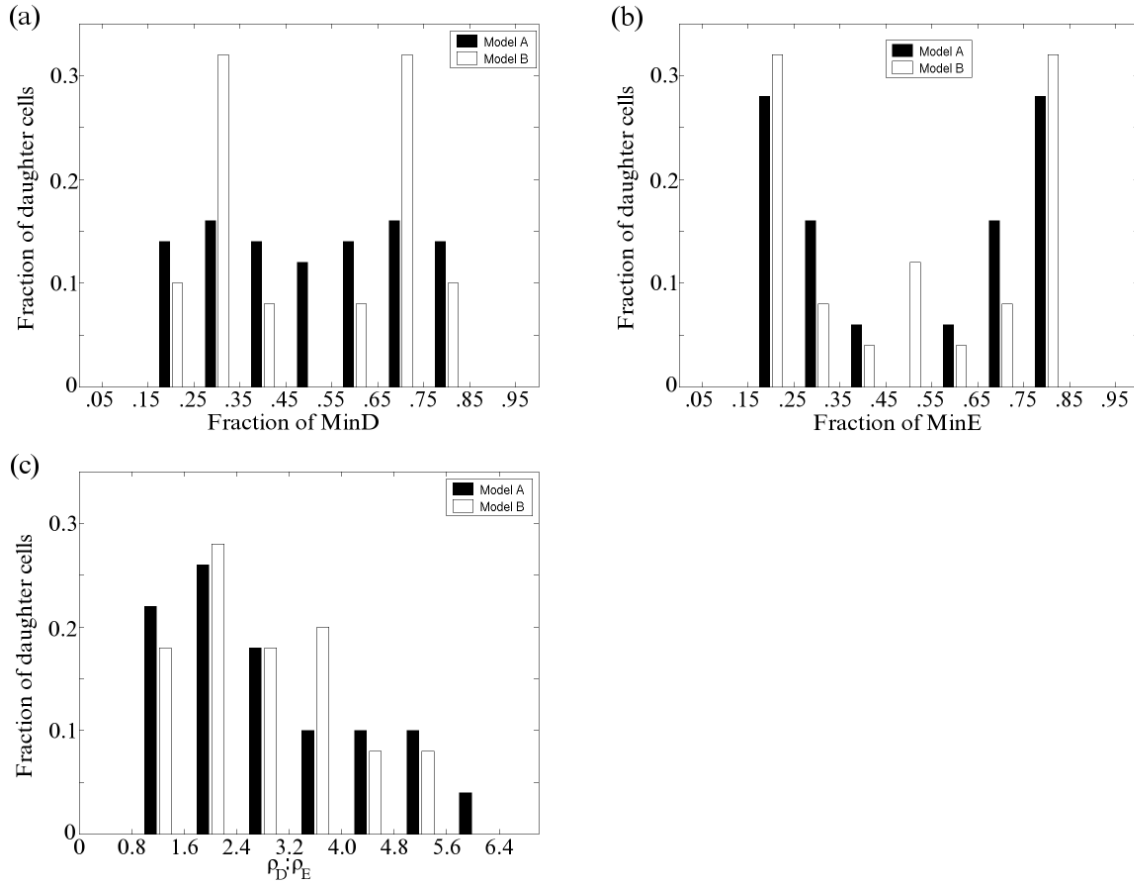


Figure 10. Comparison of the division models A and B, showing the distributions of the fraction of (a) MinD molecules and (b) MinE molecules from the parent cell, and (c) of $\rho_D : \rho_E$ ratios, in the daughter cells.

region extends only over a few sites at the centre of the cell and appears much later during division. Again this is due to the greater diffusion rates in model B.

Protein numbers in the daughter cells vary from 85% to 15% of the total in the parent cell for both MinD and MinE. This range is the same as the variation in protein numbers in each half of the parent cell during normal pole-to-pole oscillations. Figure 10 compares the daughter cell distributions between the two models. In both cases, the MinE distribution peaks at high and low concentrations. In model A, an equal distribution into the two daughter cells is never observed. The $\rho_D : \rho_E$ ratios in daughter cells are also similar in the two models. Only the MinD distribution shows a significant difference between the two models. In model A, all concentrations are approximately equally likely. In model B, however, copy numbers in the daughter cells between 25-35% and 65-75% of the total from the parent cell are strongly favoured and a 50%-50% split is never observed.

The $\rho_D : \rho_E$ ratio in daughter cells ranges from about 1.3 to 6. Those daughter cells with $\rho_D : \rho_E < 1.6$, approximately 20% of the total produced in our simulations, cannot support pole-to-pole oscillations because MinD is unable to form sufficiently

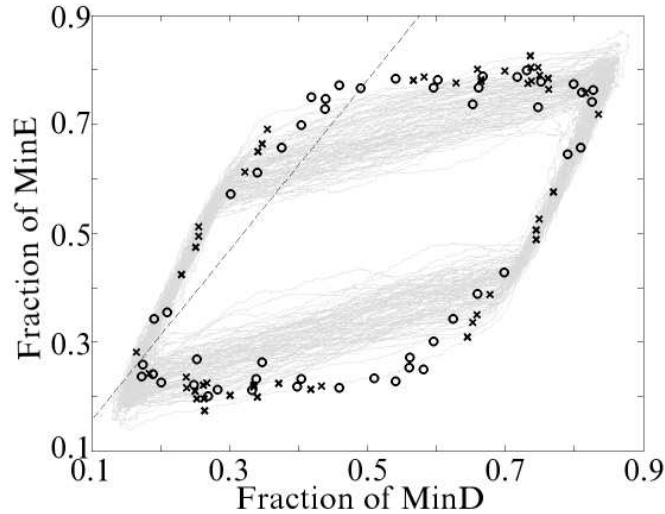


Figure 11. Points show the fraction of MinE from the parent cell in each daughter cell plotted against the fraction of MinD in the same cell. After division, these fractions are of course constant for each daughter cell. Circles represent model A, and crosses model B. The gray lines show the fraction of each protein in one half of the parent cell as a function of time during pole-to-pole oscillations. This is slightly disordered due to fluctuations. The dashed line indicates $\rho_D : \rho_E = 1.6$. Daughter cells to the left of this line do not have pole-to-pole oscillations.

long filaments on the membrane. This is consistent with our results in section 2.2. All daughter cells with $\rho_D : \rho_E > 1.6$ did have Min oscillations. However when the protein copy number is low, polar zones are less dense and fluctuations become more significant in the dynamics.

If we plot the fractions of MinE and MinD in the same half of the parent cell as a function of time as pole-to-pole oscillations take place, the result is a cycle as shown in figure 11 (gray lines). During the division process, the Min protein dynamics are of course altered. Hence, as can be seen in Figure 11, the data points showing the fraction of the proteins ending up in the daughter cells lie on another closed loop which is similar, though not identical to, the cycle of the parent cell. We can also see that both models A and B produce daughter cells with protein fractions that lie on the same closed loop.

3.2. Robustness

The results presented above appear to be general and are qualitatively the same under a number of changes (discussed below) to the division models. No systematic trends were observed when varying any of the parameters in either of the models. In fact when additional data from these perturbed models is added to the data from figure 11, all the data points continue to lie on the same loop (see figure 12).

Width of contracting region: Increasing w means that the pole-to-pole oscillations of the parent cell are disrupted sooner, because the cumulative probability of diffusion from one half of the cell to the other is reduced. Conversely, if w is reduced oscillations

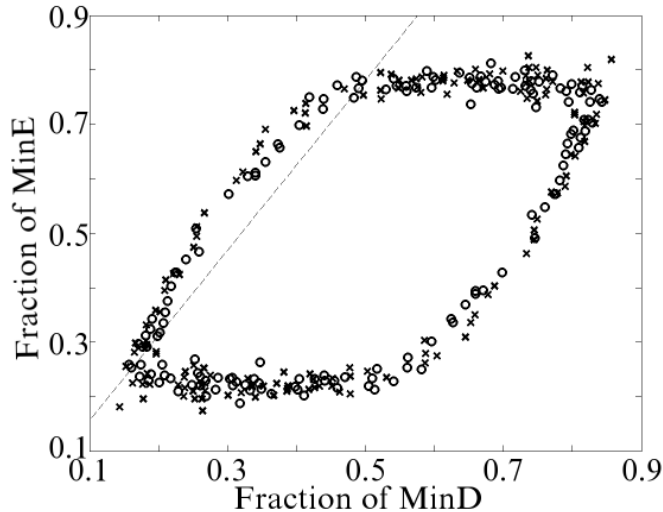


Figure 12. As for figure 11, but with data added for different w and T values and different functional time dependences.

in the parent cell will continue later into the division process. However there is no obvious effect on the protein numbers in the daughter cells when w is increased to 20 or reduced to 5.

We have also tested the case where diffusion is reduced only when crossing from one half of the cell to the other, a limiting case of our earlier models. The observed distribution of protein numbers into the daughter cells is again the same.

Form of time-dependence: We have tested model B with $r(y,t)$ decreasing quadratically with t , and model A with linear time dependence. Again the behaviour is qualitatively the same. The time at which oscillations cease is earlier if the diffusion probability decreases more rapidly with t , and later if the diffusion probability decreases more slowly. However the distributions of the Min proteins into the daughter cells are unaffected.

Division time, T : Again the distribution of Min proteins into the daughter cells showed no systematic changes. The time at which the oscillations in the parent cell ceased appeared to vary linearly with T , so it always occurred at a particular value for the diffusion probability D' or D_w . $T = 150s$ and $T = 450s$ were tested in addition to $T = 300s$.

Stochastic vs. continuous models: We also implemented a similar mechanism to model A into continuous partial differential equation models adapted from [8] and [11]. The results obtained were qualitatively the same as those shown above. This indicates that the observed behaviour is not a result of the stochastic nature of our model.

4. Conclusion and Outlook

In this paper we have introduced a new model for the Min protein oscillations, incorporating both membrane polymerisation and stochasticity. As we have seen, the

model is able to account for much of the observed Min dynamics. We have also applied our model to the dynamics of the Min proteins during cell division and found that diffusion alone is insufficient to equalise the protein copy numbers between the two daughter cells.

Although there have been a few comments on Min dynamics in constricting cells, there have been no experiments looking systematically and quantitatively at protein dynamics in large numbers of cells undergoing the division process. We hope that future experiments will investigate the partitioning of the Min proteins and follow the Min oscillations into the daughter cells. Although the results we have presented appear to be general and independent of the division mechanism, it is possible that other models would produce different behaviour. This provides potentially another way to test these models against experimental observations and each other.

The reports of oscillations in constricting cells [3, 4] have stated that oscillations of the Min proteins continue unaffected well into the division process. After this time, oscillations occur separately between each pole and mid-cell, and continue once the daughter cells have separated. These features are reproduced in our simulations - oscillations cut off sharply at some time during the closing of the septum, after which the daughter cells are effectively independent even though they have not yet completely separated.

Our simulations suggest that the distribution of the Min proteins is very often unequal and often largely skewed to one daughter cell. The variation of periods observed *in vivo* also leads us to believe that there is some variation of copy number between cells. However, in the most extreme cases of our simulations, Min oscillations are not supported in the daughter cells. Wild-type *E. coli* without pole-to-pole Min oscillations have not been reported in the literature. It may be that our model cannot reproduce oscillations at the extremes of the range where they can occur *in vivo*. However, in these cases the period of oscillation would probably lie well outside the range typically observed. This suggests that, at least in these extreme cases, some additional way of regulating protein numbers in the daughter cells may be required.

For most cytoplasmic proteins that are present in high numbers, diffusion effectively distributes them evenly throughout the cell so that at division the number in each daughter cell is roughly equal. The dynamics of the Min proteins, however, means that the distributions are normally skewed greatly towards one end of the cell. From our simulations we conclude that diffusion through the septum is not by itself able to equalise the Min protein numbers in each daughter cell.

The final expression levels in the daughter cells appear to be entirely uncorrelated with the fractions of proteins in each half of the parent cell at the beginning of the division process. This is presumably a result of the inherently stochastic nature of the model dynamics. This means it is unlikely that the initiation of division can be controlled to coincide with a certain point in the Min cycle to ensure equal $\rho_D : \rho_E$ ratios in the daughter cells. An alternative would be some form of active transport through the closing septum. This also appears unlikely, and there is certainly no experimental

evidence for such a mechanism. It therefore seems improbable that the protein numbers are regulated by the division mechanism itself, which leaves open the possibility that levels are corrected shortly after division.

In our simulations, those cells which did not have Min oscillations had a $\rho_D : \rho_E$ ratio below 1.6. This could be rectified by producing more MinD shortly after division. Additionally those cells with a very low copy number of both proteins had small and low-density polar zones, where fluctuations had a much more significant impact on the pole-to-pole oscillations, leading to a much less pronounced MinD mid-cell concentration minimum. These cells would also benefit from increased copy numbers of both proteins. This could be achieved if the production rate of the Min proteins is controlled according to their concentrations, without needing a direct trigger from the division event. The production of the Min proteins has yet to be studied experimentally, so it is not known which, if any, factors affect their production rates.

Previous studies [27, 28] have found that there is no evidence for cell-cycle dependent protein synthesis in *E. coli*, including cell division proteins such as FtsZ and FtsA. For proteins involved in the division machinery such as FtsZ, a constant production rate is sufficient for these proteins to be equally distributed at cell division. The majority of FtsZ is cytoplasmic and so the concentration throughout the parent cell would be largely equalised by diffusion. The remaining FtsZ is located at the septum in the “Z-ring”, and proteins in this structure could easily be equally divided between the daughter cells.

However, as described above, the situation for the Min proteins is likely to be rather different. Potentially the concentration levels of the Min proteins may feedback to their production (or even degradation) rates, so that, for example, their rates of synthesis increase whenever their concentrations are low. After division some cells would therefore have a burst of protein synthesis, but this would not be directly triggered due to the cell having recently divided. As the cell continues to grow the same mechanism could also keep the Min protein concentrations roughly constant. In future experiments it will be interesting to thoroughly test some of these possibilities.

Acknowledgments

We thank J. Lutkenhaus for a useful discussion. F.T. is supported by the EPSRC, and M.H. by The Royal Society.

Glossary

ATP hydrolysis: Highly exothermic chemical reaction which is a major source of energy inside a cell. MinE stimulates the hydrolysis of ATP associated with polymerised MinD, which leads to polymer disassembly.

Cell cycle: The sequence of events a cell goes through in order to reproduce, including DNA replication and division.

Pattern formation: Appearance in an extended system of spatially- and/or time-varying structures.

Reaction-diffusion system: A system of particles, each of which moves by diffusion, and where reactions occur when particles meet. These systems can sometimes display pattern formation.

Filamentous cell: A cell which is prevented from dividing, usually by removal of FtsZ, and which therefore grows much longer than is typical in wild-type bacteria.

References

- [1] Howard M and Kruse K 2005 Cellular organization by self-organization: mechanisms and models for Min protein dynamics *J. Cell Biol.* **168** 533–6
- [2] Yu X C and Margolin W 1999 FtsZ ring clusters in *min* and partition mutants: role of both the Min system and the nucleoid in regulating FtsZ ring localization *Mol. Microbiol.* **32** 315–26
- [3] Raskin D M and de Boer P A J 1999 Rapid pole-to-pole oscillation of a protein required for directing division to the middle of *Escherichia coli* *Proc. Nat. Acad. Sci. USA* **96** 4971–6
- [4] Hu Z and Lutkenhaus J 1999 Topological regulation of cell division in *Escherichia coli* involves rapid pole to pole oscillation of the division inhibitor MinC under the control of MinD and MinE *Mol. Microbiol.* **34** 82–90
- [5] Fu X, Shih Y L, Zhang Y and Rothfield L I 2001 The MinE ring required for proper placement of the division site is a mobile structure that changes its cellular location during the *Escherichia coli* division cycle *Proc. Nat. Acad. Sci. USA* **98** 980–5
- [6] Hale C A, Meinhardt H and de Boer P A J 2001 Dynamic localization cycle of the cell division regulator MinE in *Escherichia coli* *EMBO J.* **20** 1563–72
- [7] Meinhardt H and de Boer P A J 2001 Pattern formation in *Escherichia coli*: A model for the pole-to-pole oscillations of Min proteins and the localization of the division site *Proc. Nat. Acad. Sci. USA* **98** 14202–7
- [8] Howard M, Rutenberg A D and de Vet S 2001 Dynamic Compartmentalization of Bacteria: Accurate Division in *E. Coli* *Phys. Rev. Lett.* **87** 278102
- [9] Kruse K 2002 A Dynamic Model for Determining the Middle of *Escherichia coli* *Biophys. J.* **82** 618–27
- [10] Howard M and Rutenberg A D 2003 Pattern Formation inside Bacteria: Fluctuations due to the Low Copy Number of Proteins *Phys. Rev. Lett.* **90** 128102
- [11] Huang K C, Meir Y and Wingreen N S 2003 Dynamic structures in *Escherichia coli*: Spontaneous formation of MinE rings and MinD polar zones *Proc. Nat. Acad. Sci. USA* **100** 12724–8
- [12] Lackner L L, Raskin D M and de Boer P A J 2003 ATP-Dependent Interactions between *Escherichia coli* Min Proteins and the Phospholipid Membrane In Vitro *J. Bacteriol.* **185** 735–49
- [13] Hu Z, Gogol E P and Lutkenhaus J 2002 Dynamic assembly of MinD on phospholipid vesicles regulated by ATP and MinE *Proc. Nat. Acad. Sci. USA* **99** 6761–6
- [14] Suefujii K, Valluzzi R and RayChaudhuri D 2002 Dynamic assembly of Mind into filament bundles modulated by ATP, phospholipids, and MinE *Proc. Nat. Acad. Sci. USA* **99** 16776–81
- [15] Huang J, Cao C and Lutkenhaus J 1996 Interaction between FtsZ and inhibitors of cell division *J. Bacteriol.* **178** 5080–5
- [16] Hu Z, Mukherjee A, Pichoff S and Lutkenhaus J 1999 The MinC component of the division site selection system in *Escherichia coli* interacts with FtsZ to prevent polymerization *Proc. Nat. Acad. Sci. USA* **96** 14819–24
- [17] Raskin D M and de Boer P A J 1999 MinDE-Dependent Pole-to-Pole Oscillation of Division Inhibitor MinC in *Escherichia coli* *J. Bacteriol.* **181** 6419–24
- [18] Shih Y L, Le T and Rothfield L I 2003 Division site selection in *Escherichia coli* involves dynamic

- redistribution of Min proteins within coiled structures that extend between the two cell poles *Proc. Nat. Acad. Sci. USA* **100** 7865–70
- [19] Drew D A, Osborn M J and Rothfield L I 2005 A polymerization-depolymerization model that accurately generates the self-sustained oscillatory system involved in bacterial division site placement *Proc. Nat. Acad. Sci. USA* **102** 6114–8
- [20] Meacci G and Kruse K 2005 Min-oscillations in *Escherichia coli* induced by interactions of membrane-bound proteins *PB* **2** 89–97
- [21] Pavin N, Paljetak H Č and Krstić V 2005 Min Oscillation in *Escherichia coli* with Spontaneous Formation of Two-Stranded Filaments in 3D Stochastic Reaction-Diffusion Model *Preprint* arxiv:q-bio.SC/0505051
- [22] Doubrovinski K and Howard M 2005 Stochastic model for Soj relocation dynamics in *Bacillus subtilis* *Proc. Nat. Acad. Sci. USA* **102** 9808–13
- [23] King G F, Roland S L, Pan B, Mackay J P, Mullen G P and Rothfield L I 1999 The dimerization and topological specificity functions of MinE reside in a structurally autonomous C-terminal domain *Mol. Microbiol.* **31** 1161–9
- [24] Shih Y L, Fu X, King G F, Le T and Rothfield L I 2002 Division site placement in *E.coli*: mutations that prevent formation of the MinE ring lead to loss of the normal midcell arrest of growth of polar MinD membrane domains *EMBO J.* **21** 3347–57
- [25] Elowitz M B, Surette M G, Wolf P E, Stock J B and Leibler S 1999 Protein Mobility in the Cytoplasm of *Escherichia coli* *J. Bacteriol.* **181** 197–203
- [26] Lutkenhaus J 1993 FtsZ ring in bacterial cytokinesis *Mol. Microbiol.* **9** 403–9
- [27] Rueda S, Vicente M and Mingorance J 2003 Concentration and Assembly of the Division Ring Proteins FtsZ, FtsA, and ZipA during the *Escherichia coli* Cell Cycle *J. Bacteriol.* **185** 3344–51
- [28] Arends S J R and Weiss D S 2003 Inhibiting Cell Division in *Escherichia coli* Has Little If Any Effect on Gene Expression *J. Bacteriol.* **186** 880–4